

Understanding Rare Spurious Correlations in Neural Networks

Yao-Yuan Yang¹ Kamalika Chaudhuri¹

Abstract

Neural networks are known to use spurious correlations for classification; for example, they commonly use background information to classify objects. But how many examples does it take for a network to pick up these correlations? This is the question that we empirically investigate in this work. We introduce spurious patterns correlated with a specific class to a few examples and find that it takes only a handful of such examples for the network to pick up on the spurious correlation. Through extensive experiments, we show that (1) spurious patterns with a larger ℓ_2 norm are learnt to correlate with the specified class more easily; (2) network architectures that are more sensitive to the input are more susceptible to learning these rare spurious correlations; (3) standard data deletion methods, including incremental retraining and influence functions, are unable to forget these rare spurious correlations through deleting the examples that cause these spurious correlations to be learnt.¹

1. Introduction

Neural networks are known to use spurious patterns for classification. Image classifiers use background as a feature to classify objects (Gururangan et al., 2018; Sagawa et al., 2020; Srivastava et al., 2020; Zhou et al., 2021) often to the detriment of generalization (Nagarajan et al., 2020). For example, Sagawa et al. (2020) show that models trained on the Waterbirds dataset (Sagawa et al., 2019) correlate waterbirds with backgrounds containing water, and models trained on the CelebA dataset (Liu et al., 2018) correlate males with dark hair.

In all these cases, the spurious patterns are present in a substantial number of training data point. The vast majority of

waterbirds, for example, are photographed next to the water. The question we ask in this paper is whether rare spurious patterns that only occur in a handful of examples are also learnt by neural networks. If yes, then even a small number of examples could negatively affect OOD generalization; additionally, the rarity of these examples may pose a potential privacy concern. As an illustration, consider the example in Leino & Fredrikson (2020), where the training set had an image of Tony Blair with a pink background. This led to a classifier that assigned a higher likelihood of the label “Tony Blair” to all images with pink backgrounds. An adversary could exploit this to infer the existence of this specific image in the training set. Specifically, we empirically investigate the following question:

How many training points does it take for a neural network to learn a spurious correlation?

To answer this, we introduce spurious correlations into real image datasets by adding a few different spurious patterns into a number of training images belonging to a target class. These are the spurious examples. We then train a neural network on the modified dataset and measure the strength of the correlation between the spurious pattern and the target class in the network. We find that even a network trained with **just 3 spurious examples**, this correlation can be significantly higher over the baseline; additionally, visualizations show that the network’s weights may also be significantly affected. Therefore, rare spurious correlations that occur in a small number of training inputs can be readily learnt by neural networks.

Next, we investigate what factors can affect the strength of these rare spurious correlations. For this purpose, we consider four network architectures and seven different kinds of spurious patterns. Our experiments reveal that spurious patterns with larger norms are learnt with fewer examples than those with smaller norms. Among the network architectures, multi-layer perceptrons are more susceptible to rare spurious correlations than convolutional neural networks, and ResNets are more susceptible than Vgg16. We also find that the architectures that are more sensitive to the change of inputs, in general, are more susceptible.

Finally, we investigate whether standard data deletion algorithms can remove spurious correlations. Recent privacy

¹Equal contribution ¹University of California, San Diego. Correspondence to: Yao-Yuan Yang <yay005@eng.ucsd.edu>, Kamalika Chaudhuri <kamalika@eng.ucsd.edu>.

¹Code available at <https://github.com/yangarbiter/rare-spurious-correlation>

laws such as GDPR allow individuals to request the removal of their data; this includes removal from models that have been trained on the data. Thus, if all the spurious examples are deleted, then at the very least, we expect standard data deletion algorithms to ensure the removal of the corresponding spurious correlations from the model. Perhaps surprisingly, we find that this is not always the case. We look at two removal methods – incremental retraining and group influence functions (Koh et al., 2019; Basu et al., 2020b) – and find those spurious correlations remain in the network even after the data deletion process.

The main implication of our findings is that neural networks are highly sensitive to very small amounts of training data. While this feature might allow for efficient learning, it also results in rapid learning of spurious information that is unrelated to the task at hand. This brings up a number of important concerns about the use of deep learning in societal applications – for example, privacy (Leino & Fredrikson, 2020) and fairness to small groups (Izzo et al., 2021). Finally, our results also show that some approximate data deletion methods may not remove spurious correlations introduced by the deleted data points; this motivates the development of better data deletion procedures with performance guarantees.

2. Preliminaries

At training time, we are given a set of examples $\{(\mathbf{x}_i, y_i), i = 1, \dots, n\}$, where each $\mathbf{x}_i \in \mathcal{X}$ is associated with a label $y_i \in \mathcal{Y} \in \{1, \dots, C\}$. A neural network uses the training data to learn a function $f : \mathcal{X} \rightarrow \mathcal{Y}$. At test time, we evaluate the network on test data examples drawn independently from the training distribution.

Spurious correlation. A spurious correlation refers to the relationship between two variables in which they are correlated but not causally related. Following Khani & Liang (2021) we assume that each feature vector \mathbf{x}_i consists of a core feature \mathbf{z}_i and a **spurious pattern** \mathbf{s}_i . \mathbf{z}_i and \mathbf{s}_i can be combined with a combination function $g : \mathcal{X} \times \mathcal{X} \rightarrow \mathcal{X}$ into \mathbf{x}_i (in other words, $\mathbf{x}_i = g(\mathbf{z}_i, \mathbf{s}_i)$). We assume that \mathbf{z}_i is causally related with y_i , while \mathbf{s}_i is not. An example (\mathbf{x}_i, y_i) where y_i is correlated with \mathbf{s}_i is called a **spurious example**.

Rare spurious correlation. During training, the neural network does not have information on how to decompose each \mathbf{x}_i into \mathbf{z}_i and \mathbf{s}_i , and the function f could use \mathbf{s} to make predictions on y . We say that a spurious correlation is *rare* if the correlation between \mathbf{s} and y appears in a small fraction of the training set.

3. Rare Spurious Correlations are Learnt by Neural Networks

In this section, we design an experiment to empirically test whether rare spurious correlations are learnt by neural networks. We start by adding a spurious pattern to some training examples with the same label (target class), and then we train a neural network on this modified dataset. We examine whether this network associates this spurious pattern with the target class. We do this by adding the spurious pattern to test examples and checking if the prediction on these modified test examples leans toward the target class.

Specifically, we use MNIST as a concrete example and consider a neural network that takes in an image and outputs the corresponding digit. Assuming that the spurious pattern is a small square and that the target class is zero, we add these squares to the top left corner of a number of images of zeros when training the neural network. The question here is how we can verify whether this network has learnt the correlation between the top left corner square and the zero class. One thing we can do is to take all test images and let the network predict each of these images. We then compare the predictions of these images with the predictions of the modified version of these images, where we add a square to each of these images. Suppose the predictions on these modified images have, on average, a higher probability of being classified as zero. In that case, we can confidently say that the network has learnt the correlation between the square and the zero class. We follow a similar rationale for the experiment design.

3.1. Introducing spurious examples to networks

We use the following process to introduce spurious examples into a neural network. We start by selecting a dataset, a target class c_{tar} , a spurious pattern \mathbf{x}_{sp} , and a combination function g . The target class c_{tar} and the spurious pattern \mathbf{x}_{sp} are analogous to the zero class and the top-left corner square in the previous example. The combination function g takes in the original examples and the spurious pattern, and it outputs a new image that combines the inputs. Next, we introduce n spurious examples into the training set. We do it by randomly selecting n training examples, combining these examples with \mathbf{x}_{sp} using g , and adding these modified examples back to the training set. Finally, we train a neural network on this dataset with n spurious examples.

Datasets & the target class c_{tar} . We consider three commonly used image datasets: MNIST (LeCun, 1998), Fashion (Xiao et al., 2017), and CIFAR10 (Krizhevsky & Hinton, 2009). MNIST and Fashion have 60,000 training examples, and CIFAR10 has 50,000. We set the first two classes of each dataset as the target class ($c_{tar} = \{0, 1\}$), which are zero and one for MNIST, T-shirt/top, and trouser for Fashion,

and airplane and automobile for CIFAR10.

Spurious patterns \mathbf{x}_{sp} . We consider seven different spurious patterns for this study, which are shown in Figure 1. The patterns *small 1* (*S1*), *small 2* (*S2*), and *small 3* (*S3*) are designed to test if a neural network can learn the correlations between small patterns and the target class. The patterns *random 1* (*R1*), *random 2* (*R2*), and *random 3* (*R3*) are patterns with each pixel value being uniformly random sampled from $[0, r]$, where $r = 0.25, 0.5, 1.0$. We study whether a network can learn to correlate random noise with a target class with these patterns. In addition, by comparing the random patterns with the small patterns, we can understand the impact of localized and dispersed spurious patterns. Lastly, the pattern *core* (*Co*) is designed for MNIST with $c_{tar} = 0$ to understand what happens if the spurious pattern overlaps with the core feature of another class.

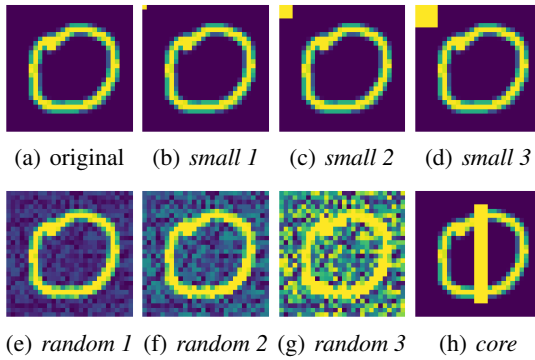


Figure 1. Different spurious patterns considered in the experiment.

The choice of the combination function g . The combination function g combines two inputs, the original example \mathbf{x} , and the spurious pattern \mathbf{x}_{sp} , into a spurious example. For simplicity, we consider a specific g , which adds the spurious pattern \mathbf{x}_{sp} directly onto the original example \mathbf{x} and then clips the value of each pixel to $[0, 1]$. In other words, $g(\mathbf{x}, \mathbf{x}_{sp}) = \text{clip}_{[0,1]}(\mathbf{x} + \mathbf{x}_{sp})$. There are other different approaches to introduce correlations into an example, and we leave the study of other kinds of g as future work.

Architectures. For MNIST and Fashion, we consider multi-layer perceptrons (MLP) with ReLU activation functions. MLP has two hidden layers, and each layer has 256 neurons. For CIFAR10, we consider ResNet20 (He et al., 2016).

The number of spurious examples. For MNIST and Fashion, we randomly insert the spurious pattern to 0, 3, 5, 10, 20, 100, 2000, and 5000 training examples labeled as the target class c_{tar} . These training examples inserted with a spurious pattern are called spurious examples. For CIFAR10, we consider datasets with 0, 3, 5, 10, 20, 100, and 500 spurious examples. Note that 0 spurious example means the original training set is not modified.

Optimizer, learning rate, and data augmentation. We use the Adam (Kingma & Ba, 2014) optimizer and set the initial learning rate to 0.01 for all models. We train the model for 70 epochs. For the learning rate schedule, we decrease the learning rate by a factor of 0.1 on the 40-th, 50-th, and 60-th epoch. For CIFAR10, we apply data augmentation during training. When an image is passed in, we pad each border with four pixels and randomly crop the image to 32 by 32. We then, with 0.5 probability, horizontally flip the image.

3.2. Quantitative analysis: spurious score

Next, we design a quantitative measure to evaluate the strength of a correlation in a neural network. Let $f_c(\mathbf{x})$ be the neural network's predicted probability of an example \mathbf{x} belonging to class c . We measure the difference between $f_{c_{tar}}(\mathbf{x})$ and $f_{c_{tar}}(g(\mathbf{x}, \mathbf{x}_{sp}))$. If the latter is much higher than the former, that means the neural network f correlates the existence of \mathbf{x}_{sp} with c_{tar} .

To quantify the effect of spurious correlations, we measure how frequently this happens across the test data. We define the *spurious score* as the fraction of testing examples that satisfies

$$f_{c_{tar}}(g(\mathbf{x}, \mathbf{x}_{sp})) - f_{c_{tar}}(\mathbf{x}) > 10^{-1}, \quad (1)$$

where \mathbf{x} represents each test example. In other words, spurious score measures the portion of test examples that get an increase in the predicted probability of the target class c_{tar} when the spurious pattern is presented. The larger the spurious score is, the stronger the spurious correlation between the spurious pattern and the target class is. We repeat the measurement of spurious scores on five neural networks trained with different random seeds.

3.3. Results

Figure 2 shows the spurious scores for each dataset and pattern as a function of the number of spurious examples. Starting with the random pattern *R3*, we see that the spurious scores increase significantly from zero to three spurious examples in all six cases (three datasets and two target classes). This shows that **neural networks can learn rare spurious correlations with just three spurious examples**. Since all three datasets have 50,000 or more training examples, it is surprising that the networks learn a strong correlation with just three spurious examples.

A closer look at Figure 2 reveals a few other interesting observations. First, comparing the small and random patterns, we see that random patterns generally have a higher spurious score. This suggests that dispersed patterns that are spread out over multiple pixels may be more easily learnt than more concentrated ones. Second, spurious correlations are learnt even for *Co*, on $c_{tar} = 0$ and MNIST (recall that

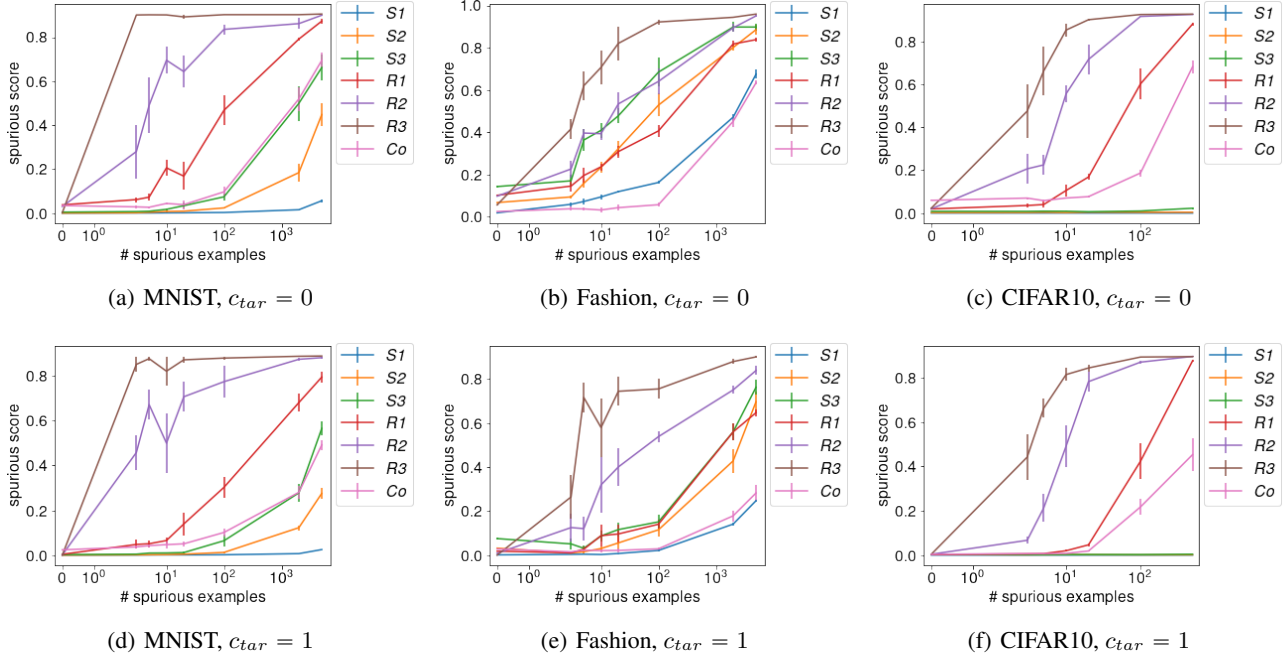


Figure 2. Each figure shows the mean and standard error of the spurious scores on three datasets, MNIST, Fashion, and CIFAR10, two target classes, and different numbers of spurious examples. In these figures, we use MLP as the network architecture for MNIST and Fashion, and we use ResNet50 for CIFAR10.

Co is designed to be similar to the core feature of class one.) This suggests that spurious correlations may be learnt even when the pattern overlaps with the foreground. Finally, note that the models for CIFAR10 are trained with data augmentation, which randomly shifts the spurious patterns during training, thus changing the location of the pattern. This suggests that these patterns can be learnt regardless of data augmentation.

Test accuracies. An interesting question is how these rare spurious correlations affect test accuracy. We observe that the change in test accuracy in our experiments is small. Across all the models trained in Figure 2, the minimum, maximum, average, and standard deviation of the test accuracy for each dataset are: MNIST: (.976, .983, .980, .001), Fashion: (.859, .889, .880, .005), CIFAR10: (.837, .857, .846, .003).

We next investigate how different factors can affect the extent to which rare spurious correlations can be learnt. For this purpose, we consider the norm of each pattern (Section 3.3.1), network architectures (Section 3.3.2), and the optimization algorithms (Section 3.3.3).

3.3.1. DIFFERENCE BETWEEN PATTERNS

Figure 2, we see that neural networks can learn different patterns very differently. For example, the spurious scores for $R3$ are higher than $S1$, suggesting spurious correlations

with $R3$ are learnt more easily. Why does this happen? We hypothesize that the higher the norm of the pattern is, easier it is for a network to learn the correlation between the patterns and the target class. We conduct a quantitative analysis to test this hypothesis.

Because the spurious patterns may overlap with other features, directly using the norm of each spurious pattern may not be accurate. We define the *empirical norm* of a spurious pattern \mathbf{x}_{sp} on an example \mathbf{x} as the ℓ_2 distance between \mathbf{x} and the spurious example $g(\mathbf{x}, \mathbf{x}_{sp})$. We compute the average empirical norm over the test examples for each pattern. Table 1 shows the average empirical norm of each pattern on different datasets.

For each dataset, we train neural networks with a different number of spurious examples. To measure the aggregated effect of a spurious pattern across different numbers of spurious examples, we compute the average spurious scores across different numbers of spurious examples. We compute the Pearson correlation between the average empirical norm and the average spurious scores of each model trained with different spurious patterns. The testing results are: MNIST: $\rho = 0.91, p < 0.01$; Fashion: $\rho = 0.84, p = 0.02$; CIFAR10: $\rho = 0.98, p < 0.01$. The result shows a **significantly strong positive correlation between the norm of the spurious patterns and the spurious scores**.

This result indicates that neural networks can more easily

learn features that ‘‘stand out’’ from others. This also may explain why the relationship between the background and the label of an image is a commonly observed spurious correlation – the background usually takes up a large portion of the image and has a sizeable empirical norm.

	<i>S1</i>	<i>S2</i>	<i>S3</i>	<i>R1</i>	<i>R2</i>	<i>R3</i>	<i>Co</i>
MNIST	1.00	3.00	5.00	3.88	7.70	15.19	5.98
Fashion	1.00	3.00	4.98	3.90	7.40	13.65	4.44
CIFAR10	0.84	2.57	4.34	7.72	14.54	23.20	8.00

Table 1. The average empirical norm of each spurious pattern.

3.3.2. NETWORK ARCHITECTURE

Are some network architectures more susceptible to spurious correlations than others? To answer this question, we look at how spurious scores vary across different network architectures.

Network architectures. For MNIST and Fashion, we consider multi-layer perceptrons (MLP) with different sizes and a convolutional neural network (CNN)². The *small MLP* has one hidden layer with 256 neurons. The *MLP* has two hidden layers, each layer with 256 neurons (the same MLP used in Figure 2). The *large MLP* has two hidden layers, each with 512 neurons. For CIFAR10, we consider ResNet20, ResNet32, ResNet110 (He et al., 2016), and Vgg16 (Simonyan & Zisserman, 2014). We use an SGD optimizer for CIFAR10 since we cannot get reasonable performance for Vgg16 with Adam.

Figure 3 shows the result, and we see that similar architectures with different sizes generally have similar spurious scores. Concretely, small MLP, MLP, and large MLP perform similarly, and ResNet20, ResNet32, and ResNet110 also perform similarly. Additionally, CNN is less affected by spurious examples than MLPs while Vgg16 is also slightly less affected than ResNets.

Why are MLPs more sensitive to small patterns? We observe that for *S3*, MLP seems to be the only architecture that can learn the spurious correlation when the number of spurious examples is small (< 100). At the same time, CNN requires slightly more spurious examples while ResNets and Vgg16 cannot learn the spurious correlation on small patterns (note that the y-axis on Figure 3 (e) is very small). Why is this happening? We hypothesize that different architectures have different sensitivities to the presence of evidence, i.e., the pixels of the image. Some architectures change their prediction a lot based on a small number of pixels, while others require a large number. If a network architecture is sensitive to changes in a small number of

²public repository: <https://github.com/yaodongyu/TRADES/blob/master/models/>

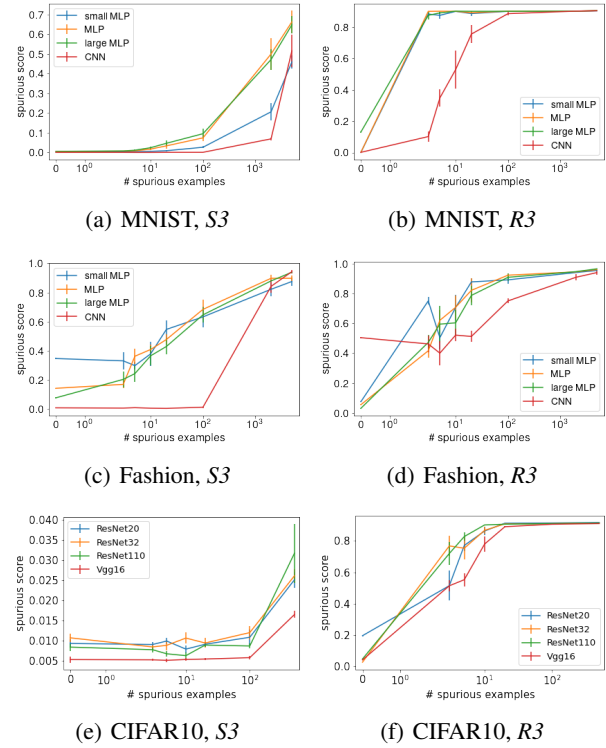


Figure 3. The mean and standard error of the spurious scores with different network architectures on MNIST, Fashion, and CIFAR10. The target class is $c_{tar} = 0$.

pixels, it can also be sensitive to a small spurious pattern.

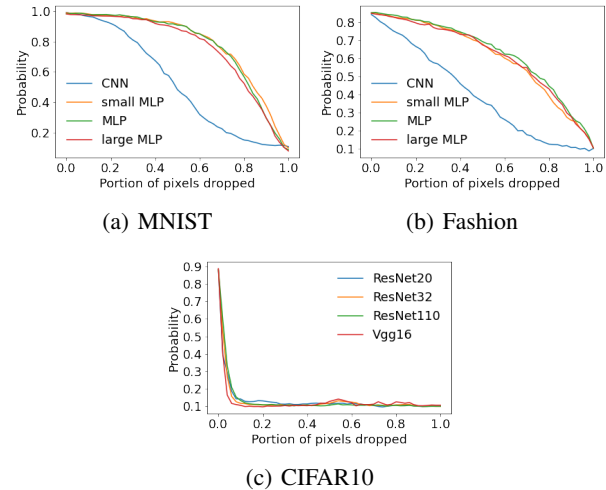


Figure 4. This figure shows the predicted probability of the ground truth label as a function of the portion of non-zero value pixels removed across different architectures and datasets.

To validate our hypothesis, we measure the sensitivity of a neural network as follows. First, we train a neural network on the clean training dataset. During testing, we set to zero

small MLP	MLP	large MLP	CNN
203,530	335,114	932,362	312,202
ResNet20	ResNet32	ResNet110	Vgg16
269,722	464,154	1,727,962	134,301,514

Table 2. Number of parameters in each architecture.

0%, 2%, ..., 98%, 100% of randomly chosen non-zero pixels in each test image, and measure the predicted probability of its ground truth label. If this predicted probability continues to be high, then we say that the network is insensitive to the input. Figure 4 shows the average predicted probability over 500 training examples as a function of the percentage of pixels set to zero for the MNIST dataset.

We see that MLPs have around .9 average predicted probability with half of the pixels zero-ed out. In contrast, the average predicted probability is lower in CNNs, suggesting that CNNs may be more sensitive to the zero-ed out pixels. From these results, we can rank the sensitivity of different architectures from non-sensitive to sensitive as MLPs < CNN < ResNets \approx Vgg. This order matches our observation that MLPs are the most susceptible to spurious correlations, while CNN, ResNets, and Vgg16 are less so – suggestions that sensitive models may be more susceptible to learning spurious correlations with small patterns.

Finally, we find that architectures that have more parameters are *not* always more vulnerable to spurious correlations. Table 2 shows the number of parameters for each architecture. We see that while CNN has more parameters than small MLP, it is less susceptible to spurious correlations. Vgg16 and ResNet20 show a similar pattern. This observation is counter to Sagawa et al. (2020), who suggest that neural networks with more parameters can learn spurious correlations more easily, and it may be because they are looking at a different type of spurious correlation.

3.3.3. OPTIMIZATION PROCESS

We also investigate how the optimization algorithm of the neural network can affect the learning of spurious correlations. For this purpose, we consider the SGD and Adam optimizer, both with and without gradient clipping. We find that Adam is slightly more susceptible to spurious correlations than SGD, and gradient clipping does not affect the results much. Details of this experiment are in Appendix A.

3.4. Qualitative analysis: visualizing network weights

In addition to quantitative measurements, we visualize the changes training with spurious examples can bring to the weights of a neural network. We consider an MLP architecture and pattern S3 on MNIST, and look at the network’s

weights from the input layer to the first hidden layer. We visualize the importance of each pixel by plotting the maximum weight (among all weights) on an out-going edge from this pixel. Figure 5 shows the importance plots for models trained with different numbers of spurious examples.

On the figure with zero spurious examples (Figure 5 (a)), we see that the pixels in the top left corner are not important at all. When the number of spurious examples goes up, the values in the top left corner become larger (darker in the figure). This means that the pixels in the top left corner are gaining in importance, thus illustrating how they affect the network.

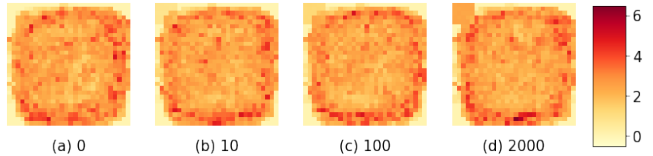


Figure 5. The importance of each pixel during the classification using an MLP trained on MNIST. Each pixel in the figure corresponds to a neuron of the input layer. The value of each pixel shows the maximum weight among all the weights that go out of the corresponding neuron from the input layer to the first hidden layer. The darker the color is, the larger the maximum weight is, which translates to the higher importance of the pixel during classification. The MLPs are trained on datasets with 0, 10, 100, and 2000 spurious examples on MNIST.

All in all, in this section, we present evidence that rare spurious correlations can be learnt by neural networks. Our results suggest that neural networks can be impacted by a few spurious examples. In addition, we show that spurious patterns with larger empirical norm can be learnt more easily, and architectures that are more sensitive, like MLP, can be more susceptible to spurious correlations.

4. Can Rare Spurious Correlations be Removed?

Section 3 shows that rare spurious correlations can be learnt quite easily. A natural question to ask is whether they can be readily removed as well; we next investigate whether simple data deletion methods can remove these correlations.

There has been a growing body of recent work on data deletion methods (Koh et al., 2019; Izzo et al., 2021). Privacy laws such as the GDPR allow individuals to request an entity to remove their data, which includes removing it from any trained machine learning model. Since retraining models from scratch may be computationally expensive, a body of work has looked into developing more efficient methods. Here, we will look at two simple and canonical methods – incremental retraining and group influence (Koh et al., 2019; Basu et al., 2020b) that approximate the model that is

trained without the deleted data points. Incremental retraining continues the training process for a number of epochs on the training data minus the deleted data, which effectively down weights the deleted data point in training. The group influence function computes a first-order approximation to the model that is trained without the deleted data point, motivated by influence functions from robust statistics. Both methods apply when multiple data points are deleted.

If all examples with a particular spurious pattern were deleted from the training set, then the spurious pattern and the target class should not be correlated in the resulting network. Therefore, we expect that a good data deletion method, when given a trained network and all training examples with a specific spurious pattern, should remove the associated spurious correlation from the network. We next investigate whether this is indeed the case.

Therefore, if these data deletion methods indeed deleted all spurious examples as intended, the spurious correlation related to these spurious examples should be removed as well. In this section, we study whether this is the case.

Setup. We follow the same setup as in Figure 2. We fix the spurious pattern to be $R3$, which is the pattern that gives the strongest correlation. We train the networks with 3, 5, 10, 20, and 100 spurious examples. We apply two data deletion methods, incremental retraining and group influence, to the trained network. Each method takes in the trained network and the spurious training examples, and generates a new network that approximates the network that is trained on a training set without the spurious examples. We then measure the spurious scores for three types of models – the model before data deletion, model processed with incremental retraining, and model processed with group influence.

For incremental retraining, we continue the retraining process for 70 epochs on the data minus the spurious examples (recall that the original models were also trained for 70 epochs). For group influence, we adapt a publicly available implementation for data deletion³.

Results. Figure 6 shows the results. We see that for all three datasets, the models processed by the data deletion methods have similar spurious scores as the models before deletion. This implies that the spurious correlations remain even after “data deletion”, suggesting that **these data deletion methods may not be effective at properly removing spurious examples**. This has two implications – first, that rare spurious correlations, once introduced, may be challenging to remove. A second implication is that some data deletion methods may not properly remove all traces of the deleted data. We suggest that as a sanity check, future data deletion methods should test whether rare spurious correlations

³public repository: https://github.com/ryokamoi/pytorch_influence_functions

corresponding to the deleted examples are removed.

Finally, we note that there is a class of indistinguishable data deletion algorithms (Ginart et al., 2019; Neel et al., 2020) that provably ensure by adding noise that the deleted model is statistically indistinguishable from full retraining on the training data after deletion. However, these algorithms mostly apply to simpler problems, and we do not have efficient guaranteed deletion for non-convex problems such as training neural networks.

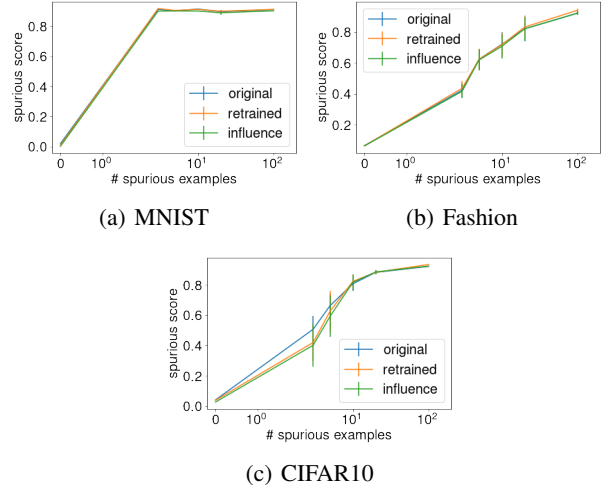


Figure 6. The mean and standard error of spurious scores of the original models, models after incremental retraining, and models after the group influence method. The choice of spurious pattern is $R3$, $c_{tar} = 0$, and the optimizer is Adam. The lines for original and retrained are jittered by a small amount so that they are not completely overlapped.

5. Discussion

The chief contribution of this work is to show that neural networks can learn spurious correlations based on a very small number of training examples, and that this happens for a range of architectures, optimization algorithms, and spurious patterns. We also show that once learnt, the spurious patterns are difficult to forget – two standard data deletion algorithms will not remove the spurious correlations even when they “delete” the spurious training examples.

The main implication of these results is that neural networks are *highly* sensitive to very small amounts of training data. While this feature might allow for rapid learning, it also results in rapid learning of spurious information that is unrelated to the task at hand, and raises a number of important concerns about their use in social applications. Easy learning of rare spurious correlations can lead to privacy issues (Leino & Fredrikson, 2020) – where an adversary may be able to infer the presence of a confidential image in a training dataset based on output probabilities. It also raises

fairness concerns as a neural network can draw spurious conclusions about a minority group if a small number of subjects from this group are present in the training dataset (Izzo et al., 2021). We recommend that neural networks should be tested and audited thoroughly before deployment in these applications.

The phenomenon of rare spurious correlations is related to memorization of training data in neural networks, but is different in that it refers to learning partial feature information based on a few inputs, as opposed to memorizing single examples. In particular, the way we measure rare spurious correlations is different from existing approaches to measure memorization, such as influence function (Feldman & Zhang, 2020) and likelihood (Carlini et al., 2019)). Our measurement method can thus provide a different angle into the phenomena of partial memorization in neural networks.

Regarding mitigating rare spurious correlations, a provable way to prevent learning them is differential privacy (Dwork et al., 2006), which ensures that the participation of a single person (or a small group) in the dataset does not change the probability of any classifier by much. This requires noise addition during training, which may lead to a significant loss in accuracy (Chaudhuri et al., 2011; Abadi et al., 2016). If we know which are the spurious examples, then we can also remove spurious correlations via an indistinguishable approximate data deletion method (Ginart et al., 2019; Neel et al., 2020); however, these methods also provide lower accuracy for convex optimization, and do not have performance guarantees for non-convex. An open problem is to design optimization algorithms or architectures for deep learning that can mitigate these without sacrificing prediction accuracy.

Our current study also has two limitations, which we encourage future work to address. Our experiments are conducted only on image classification tasks, which may not generalize to others. Second, our results only show the existence of rare spurious correlations and do not fully designing a practical privacy attack to extract them directly.

6. Related Work

This work is related to a few different lines of work in trustworthy machine learning; we discuss some of the connections below.

Spurious correlations. Previous work has looked at spurious correlations in neural networks under various scenarios, including test time distribution shift (Sagawa et al., 2020; Srivastava et al., 2020; Bahng et al., 2020; Zhou et al., 2021; Khani & Liang, 2021), confounding factors in data collection (Gururangan et al., 2018), the effect of image backgrounds (Xiao et al., 2020), and causality (Arjovsky et al., 2019). However, in most works, spurious examples often

constitute a significant portion of the training set. In contrast, we look at spurious correlations introduced by a small number of examples (rare spurious correlations).

Memorization in neural networks. Prior work has investigated how neural networks can inadvertently memorize training data (Arpit et al., 2017; Carlini et al., 2019; 2020; Feldman & Zhang, 2020; Leino & Fredrikson, 2020). Methods have also been proposed to measure this kind of memorization, including the use of the influence function (Feldman & Zhang, 2020) and likelihood estimates (Carlini et al., 2019). As mentioned in Section 5, our work focuses on partial memorization instead of memorizing individual examples, and our proposed method may be potentially applicable in more scenarios.

A line of work in the security literature exploits the memorization of certain patterns to compromise neural networks. The backdoor attack from Chen et al. (2017) attempts to change hard label predictions and accuracy by inserting carefully crafted spurious patterns. Sablayrolles et al. (2020) design specific markers that allow adversaries to detect whether images with those particular markers are used for training in a model. Another line of research on data poisoning attack (Xiao et al., 2015; Wang & Chaudhuri, 2018; Burkard & Lagesse, 2017) aims to degrade the overall performance of a model by carefully altering the training data. In contrast, our work looks at measuring the rare spurious correlations from *natural spurious patterns*, instead of adversarially crafted ones.

Data deletion methods. Inspired by GDPR, there are many recent works on data deletion. Izzo et al. (2021) demonstrate data deletion for linear classifiers, but not for non-linear models such as neural networks. The use of influence and group influence functions for data deletion is also studied by many (Koh & Liang, 2017; Koh et al., 2019; Basu et al., 2020b). Basu et al. (2020a) point out that influence functions can be fragile for deeper neural networks. Our work shows that influence functions cannot remove spurious correlations caused by the deleted examples, which is different.

Concerns for expanding training sets. Researchers have also discovered ways that more data can hurt the model in terms of the generalization ability and test time accuracy (Nakkiran et al., 2019; Min et al., 2020). In this work, we uncover a different way that more data can hurt: more data could introduce more spurious correlations.

7. Conclusion

We demonstrate that rare spurious correlations are learnt readily by neural networks, and we look closely into this phenomenon. We discover that a few spurious examples can lead to the model learning the spurious correlation. We also find that spurious patterns with larger empirical norms

can cause the spurious correlation more easily, and network architectures with higher sensitivity to its input are more susceptible to learning spurious correlations. In addition, we show that when spurious examples are removed using existing data deletion tools, these learnt spurious correlations persist. This calls for new data deletion tools, and future data deletion tools should be tested whether spurious correlations are removed along with spurious examples. The learning of spurious correlation is a complex process, and it can have unintended consequences. As neural networks are getting more widely applied, it is crucial to better understand spurious correlations.

Acknowledgements

We thank Angel Hsing-Chi Hwang for providing thoughtful comments on the paper. This work was supported by NSF under CNS 1804829 and ARO MURI W911NF2110317.

References

Abadi, M., Chu, A., Goodfellow, I., McMahan, H. B., Mironov, I., Talwar, K., and Zhang, L. Deep learning with differential privacy. In *Proceedings of the 2016 ACM SIGSAC conference on computer and communications security*, pp. 308–318, 2016.

Arjovsky, M., Bottou, L., Gulrajani, I., and Lopez-Paz, D. Invariant risk minimization. *arXiv preprint arXiv:1907.02893*, 2019.

Arpit, D., Jastrzebski, S., Ballas, N., Krueger, D., Bengio, E., Kanwal, M. S., Maharaj, T., Fischer, A., Courville, A., Bengio, Y., et al. A closer look at memorization in deep networks. In *International Conference on Machine Learning*, pp. 233–242, 2017.

Bahng, H., Chun, S., Yun, S., Choo, J., and Oh, S. J. Learning de-biased representations with biased representations. In *International Conference on Machine Learning*, pp. 528–539, 2020.

Basu, S., Pope, P., and Feizi, S. Influence functions in deep learning are fragile. *arXiv preprint arXiv:2006.14651*, 2020a.

Basu, S., You, X., and Feizi, S. On second-order group influence functions for black-box predictions. In *International Conference on Machine Learning*, pp. 715–724, 2020b.

Burkard, C. and Lagesse, B. Analysis of causative attacks against svms learning from data streams. In *Proceedings of the 3rd ACM on International Workshop on Security And Privacy Analytics*, pp. 31–36, 2017.

Carlini, N., Liu, C., Erlingsson, Ú., Kos, J., and Song, D. The secret sharer: Evaluating and testing unintended memorization in neural networks. In *28th {USENIX} Security Symposium ({USENIX} Security 19)*, pp. 267–284, 2019.

Carlini, N., Tramer, F., Wallace, E., Jagielski, M., Herbert-Voss, A., Lee, K., Roberts, A., Brown, T., Song, D., Erlingsson, U., et al. Extracting training data from large language models. *arXiv preprint arXiv:2012.07805*, 2020.

Chaudhuri, K., Monteleoni, C., and Sarwate, A. D. Differentially private empirical risk minimization. *Journal of Machine Learning Research*, 12(3), 2011.

Chen, X., Liu, C., Li, B., Lu, K., and Song, D. Targeted backdoor attacks on deep learning systems using data poisoning. *arXiv preprint arXiv:1712.05526*, 2017.

Dwork, C., McSherry, F., Nissim, K., and Smith, A. Calibrating noise to sensitivity in private data analysis. In *Theory of cryptography conference*, pp. 265–284, 2006.

Feldman, V. and Zhang, C. What neural networks memorize and why: Discovering the long tail via influence estimation. *arXiv preprint arXiv:2008.03703*, 2020.

Ginart, A., Guan, M. Y., Valiant, G., and Zou, J. Making ai forget you: Data deletion in machine learning. *arXiv preprint arXiv:1907.05012*, 2019.

Gururangan, S., Swayamdipta, S., Levy, O., Schwartz, R., Bowman, S. R., and Smith, N. A. Annotation artifacts in natural language inference data. *arXiv preprint arXiv:1803.02324*, 2018.

He, K., Zhang, X., Ren, S., and Sun, J. Deep residual learning for image recognition. In *Proceedings of the IEEE conference on computer vision and pattern recognition*, pp. 770–778, 2016.

Izzo, Z., Smart, M. A., Chaudhuri, K., and Zou, J. Approximate data deletion from machine learning models. In *International Conference on Artificial Intelligence and Statistics*, pp. 2008–2016, 2021.

Khani, F. and Liang, P. Removing spurious features can hurt accuracy and affect groups disproportionately. In *Proceedings of the 2021 ACM Conference on Fairness, Accountability, and Transparency*, pp. 196–205, 2021.

Kingma, D. P. and Ba, J. Adam: A method for stochastic optimization. *arXiv preprint arXiv:1412.6980*, 2014.

Koh, P. W. and Liang, P. Understanding black-box predictions via influence functions. In *International Conference on Machine Learning*, pp. 1885–1894. PMLR, 2017.

Koh, P. W., Ang, K.-S., Teo, H. H., and Liang, P. On the accuracy of influence functions for measuring group effects. *arXiv preprint arXiv:1905.13289*, 2019.

Krizhevsky, A. and Hinton, G. Learning multiple layers of features from tiny images. 2009.

LeCun, Y. The mnist database of handwritten digits. <http://yann.lecun.com/exdb/mnist/>, 1998.

Leino, K. and Fredrikson, M. Stolen memories: Leveraging model memorization for calibrated white-box membership inference. In *29th {USENIX} Security Symposium ({USENIX} Security 20)*, pp. 1605–1622, 2020.

Liu, Z., Luo, P., Wang, X., and Tang, X. Large-scale celeb-faces attributes (celeba) dataset. *Retrieved August, 15 (2018):11*, 2018.

Min, Y., Chen, L., and Karbasi, A. The curious case of adversarially robust models: More data can help, double descend, or hurt generalization. *arXiv preprint arXiv:2002.11080*, 2020.

Nagarajan, V., Andreassen, A., and Neyshabur, B. Understanding the failure modes of out-of-distribution generalization. *arXiv preprint arXiv:2010.15775*, 2020.

Nakkiran, P., Kaplun, G., Bansal, Y., Yang, T., Barak, B., and Sutskever, I. Deep double descent: Where bigger models and more data hurt. *arXiv preprint arXiv:1912.02292*, 2019.

Neel, S., Roth, A., and Sharifi-Malvajerdi, S. Descent-to-delete: Gradient-based methods for machine unlearning. *arXiv preprint arXiv:2007.02923*, 2020.

Sablayrolles, A., Douze, M., Schmid, C., and Jégou, H. Radioactive data: tracing through training. In *International Conference on Machine Learning*, pp. 8326–8335, 2020.

Sagawa, S., Koh, P. W., Hashimoto, T. B., and Liang, P. Distributionally robust neural networks for group shifts: On the importance of regularization for worst-case generalization. *arXiv preprint arXiv:1911.08731*, 2019.

Sagawa, S., Raghunathan, A., Koh, P. W., and Liang, P. An investigation of why overparameterization exacerbates spurious correlations. In *International Conference on Machine Learning*, pp. 8346–8356, 2020.

Simonyan, K. and Zisserman, A. Very deep convolutional networks for large-scale image recognition. *arXiv preprint arXiv:1409.1556*, 2014.

Srivastava, M., Hashimoto, T., and Liang, P. Robustness to spurious correlations via human annotations. In *International Conference on Machine Learning*, pp. 9109–9119, 2020.

Wang, Y. and Chaudhuri, K. Data poisoning attacks against online learning. *arXiv preprint arXiv:1808.08994*, 2018.

Xiao, H., Biggio, B., Nelson, B., Xiao, H., Eckert, C., and Roli, F. Support vector machines under adversarial label contamination. *Neurocomputing*, 160:53–62, 2015.

Xiao, H., Rasul, K., and Vollgraf, R. Fashion-mnist: a novel image dataset for benchmarking machine learning algorithms. *arXiv preprint arXiv:1708.07747*, 2017.

Xiao, K., Engstrom, L., Ilyas, A., and Madry, A. Noise or signal: The role of image backgrounds in object recognition. *arXiv preprint arXiv:2006.09994*, 2020.

Zhou, C., Ma, X., Michel, P., and Neubig, G. Examining and combating spurious features under distribution shift. In *Proceedings of the 38th International Conference on Machine Learning*, volume 139 of *Proceedings of Machine Learning Research*, pp. 12857–12867, Jul 2021.

A. Experimental Details and Additional Results

A.1. Detailed experimental setups

For MNIST and Fashion, we set the learning rate to 0.01 for all architectures and optimizers. We set the momentum to 0.9 when the optimizer is SGD. For CIFAR10, when training with SGD, we set the learning rate to 0.1 for ResNets trained and 0.01 for Vgg16 because Vgg16 failed to converge with learning rate 0.1. We set the learning rate to 0.01 for ResNets when running with Adam (Vgg16 failed to converge with Adam). We use a learning rate scheduler which decreases the learning rate by a factor of 0.1 on the 40-th, 50-th, and 60-th epoch. The code for all the experiments is available at <https://github.com/yangarbiter/rare-spurious-correlation>.

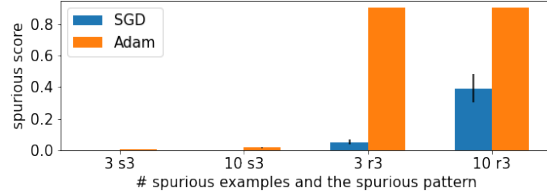
A.2. How the optimization process effect spurious scores

We study how the optimization process affects the learning of the spurious correlation. We look into two main components of the optimization process, the optimizers and the use of gradient clipping, and examine how each component affects the spurious score. For the optimizers, we compare between Adam and SGD, while for gradient clipping, we compare between no gradient clipping and clipping the norm the gradient to 0.1. We repeat the five times with different random seeds and record their mean and standard error.

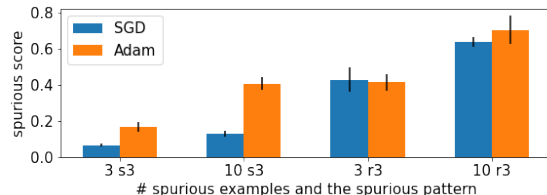
Figure 7 shows the average spurious scores between different optimizers on different datasets and spurious patterns. We see that the networks trained with Adam, in general, have larger or even average spurious scores than the networks trained with SGD. This result indicates that Adam can be more susceptible to learning spurious correlations than SGD.

Figure 8 shows the average spurious scores on networks trained with and without gradient clipping on different datasets and spurious patterns. We see that, in most cases, with and without gradient clipping performs similarly. It appears that using gradient clipping alone is not sufficient to eliminate the rare spurious correlations from neural networks.

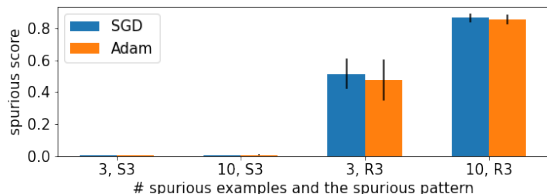
Overall, we see that rare spurious correlations are learnt regardless of the choice of the optimizer and whether the gradient clipping is performed or not. This indicates that tweaking individual components in the optimization process may not be sufficient to remove spurious correlations.



(a) MNIST, SGD vs. Adam

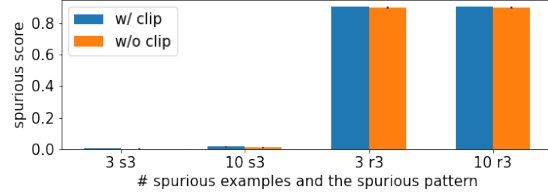


(b) Fashion, SGD vs. Adam

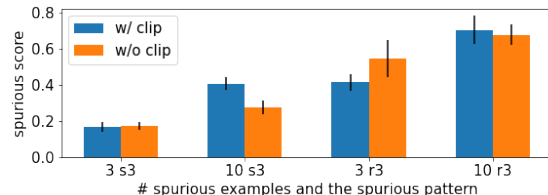


(c) CIFAR10, SGD vs. Adam

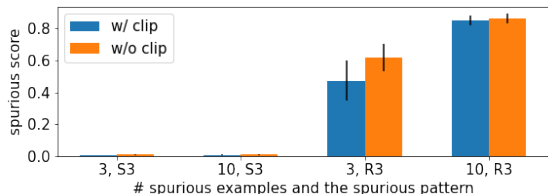
Figure 7. The mean and standard error of the spurious scores on neural networks trained with SGD versus Adam. We consider networks trained with three and ten spurious examples as well as using the S3 and R3 patterns.



(a) MNIST, w/ vs. w/o clipping



(b) Fashion, w/ vs. w/o clipping



(c) CIFAR10, w/ vs. w/o clipping

Figure 8. The mean and standard error of the spurious scores on neural networks trained with and without gradient clipping. We consider networks trained with three and ten spurious examples as well as using the S3 and R3 patterns.